

5E4000152

April 1990

LU-TP-90-5

Fractal Structures and Intermittency in QCD

Gösta Gustafson

Department of Theoretical Physics, University of Lund
Sölvegatan 14A, S-22362 Lund, Sweden

Abstract

New results are presented for fractal structures and intermittency in QCD parton showers. A geometrical interpretation of the anomalous dimension in QCD is given. It is shown that model predictions for factorial moments in the PEP-PETRA energy range are increased if the properties of directly produced pions are more carefully taken into account.

Talk presented at the Santa Fe workshop on Intermittency in High Energy Collisions, Santa Fe, March 1990

1. Introduction

The earlier results discussed in this introduction are obtained in collaboration with B. Andersson and P. Dahlqvist, while the new results in sections 2 and 3 are obtained together with the students A. Nilsson and C. Sjögren. In section 2 I will discuss properties of perturbative QCD, while in section 3 I discuss intermittent effects in soft hadronization. I concentrate on data for e^+e^- -annihilation from PEP and PETRA, but the results are relevant also to hadron collisions and DIS.

If we study e.g. e^+e^- -annihilation into hadrons, this process is often described in terms of two phases, a hard perturbative phase, described in terms of quarks and gluons, and a soft phase in which the energy of these partons is transformed into the observable hadrons. The latter phase can be described in terms of clusters or in terms of strings as in the Lund model, see fig. 1. At high energies the properties of the hard phase are most important, while the soft phase is more essential at lower energies, as will be further discussed in the following.

To study the hard perturbative phase we use two important tools:

- The dipole formulation of QCD cascades [1]
- An infrared stable measure on parton states related to the hadronic multiplicity [2]

Gluon Emission

A high energy $q\bar{q}$ -system radiates gluons according to the dipole formula

$$dn = \frac{3\alpha_s}{4\pi^2} \frac{dk_{\perp}^2}{k_{\perp}^2} dy d\varphi \quad (1)$$

Here the phase space available is given by the relation

$$|y| \lesssim \frac{1}{2} \ln(s/k_{\perp}^2) \quad (2)$$

which corresponds to the triangular region in a $y - \ln k_{\perp}^2$ diagram as shown in fig. 2a.

If two gluons are emitted, then the distribution of the hardest gluon is described by eq. (1), while the distribution of the second, softer, gluon corresponds to two dipoles,

one stretched between the quark and the first gluon, and the second between this gluon and the antiquark [3].

If the masses of the qg_1 and $g_1\bar{q}$ systems are $\sqrt{s_{12}}$ and $\sqrt{s_{23}}$ respectively, then the transverse momentum and rapidity of the first gluon are given by the relations

$$\begin{cases} s \cdot k_{\perp 1}^2 &= s_{12} \cdot s_{23} \\ y_1 &= \frac{1}{2} \ln \frac{s_{23}}{s_{12}} \end{cases} \quad (3)$$

Therefore the rapidity range Δy available for the second gluon is given by

$$\begin{aligned} \Delta y &= \ln(s_{12}/k_{\perp 2}^2) + \ln(s_{23}/k_{\perp 2}^2) = \\ &= \ln s + \ln k_{\perp 1}^2 - 2 \ln k_{\perp 2}^2 \end{aligned} \quad (4)$$

The phase space available for the second gluon thus corresponds to the folded surface in fig. 2b, with the constraint $k_{\perp 2}^2 < k_{\perp 1}^2$, as the first gluon is assumed to be the hardest one.

This procedure can be generalized so that the distribution of a third, still softer gluon corresponds to three dipoles. With n gluons the emission of gluon number $n+1$ is given by a chain of dipoles as indicated in fig. 3. We note that the dipoles connect the gluons in the same way as the string in the Lund fragmentation model.

Thus, with many gluons the gluonic phase space can be represented by the multifaceted surface in fig. 2c. Each gluon adds a fold to the surface, which increases the phase space for softer gluons.

We note that in this process the recoils are neglected, as is normal in the leading log approximation. With these approximations it is possible to make analytic calculations, as we will see below. Recoil effects and kinematical constraints for hard gluons can be taken into account in a Monte Carlo simulation program (for hard gluons the constraint in eq. (2) is not exactly correct but should be replaced by $\cosh(y) < \sqrt{s}/2k_{\perp}$). Such a program called ARIADNE is developed by U. Pettersson and L. Lönnblad [4].

Hadron production

In string fragmentation (or a longitudinal phase space model) the hadronic multiplicity for a simple $q\bar{q}$ -system is proportional to $\ln s$. The hadrons are evenly distributed in rapidity, which means that their energy-momentum four-vectors are distributed around a hyperbola (cf fig. 4a).

For a $q\bar{q}g$ -system, we obtain in the Lund string fragmentation model a bent string with two straight segments. The energy in the segments is s_{12} and s_{23} , where $s_{ij} = (k_i + k_j)^2$ and k_1, k_2 and k_3 are the momenta of the q, g and \bar{q} respectively. Thus the average multiplicity, n , is given by the relation

$$\langle n \rangle \sim \ln s_{12} + \ln s_{23} \approx \ln s + \ln k_{\perp}^2 \quad (5)$$

Here k_{\perp} is the transverse momentum of the gluon. We also note that this expression is equal to the length of the baseline of the surface in fig. 2b. The momentum distribution of the hadrons is in this case given by two hyperbolae (fig. 4b).

For a multigluon state we find in the same way

$$\langle n \rangle \sim \sum \ln(s_{i,i+1}/m_0^2) \approx \ln(s/m_0^2) + \sum \ln(k_{\perp i}^2/m_0^2) = \lambda \quad (6)$$

This expression, which we call λ , is an "effective rapidity range". It is given by the length of the baseline in fig. 2c.

It is possible to calculate the distribution $P(\lambda, s)$ in λ for fixed s [2]. We introduce the Laplace transform \mathcal{P} and use the following notation

$$\begin{aligned} L &= \ln(s/\Lambda^2) \\ \mathcal{P}(\beta, L) &= \int d\lambda e^{-\beta\lambda} P(\lambda, L) \end{aligned} \quad (7)$$

It is then possible to derive the following differential equation

$$\frac{d^2}{dL^2}(\ln \mathcal{P}(\beta, L)) = \frac{\alpha_0}{L}(\mathcal{P}(\beta, L) - 1) \quad (8)$$

where $\alpha_0/L = 3\alpha_s/2\pi$

together with the boundary conditions

$$\begin{cases} \mathcal{P}(\beta, 0) = 1 \\ \frac{d}{dL}\mathcal{P}(\beta, L=0) = -\beta \end{cases} \quad (9)$$

This implies that it is possible to obtain the **full** distribution in λ for **all** energies. (In the conventional approach to the cascade only asymptotic results are obtained [5].) Simple expressions are obtained for the first few moments, while the full distribution can be obtained by numerical calculations. Thus we find e.g.

$$\bar{\lambda} = \sqrt{\frac{L}{\alpha_0}} I_1(2\sqrt{\alpha_0 L}) \underset{s \text{ large}}{\sim} (\ln s)^{1/4} \exp(2\sqrt{\alpha_0 \ln s}) \quad (10)$$

We note that in the conventional approach the same exponential expression is obtained for the average gluon multiplicity only in a very complicated way.

The quantity λ can be generalized in an infrared stable way such that soft gluons give small but positive contributions [6]. This implies that no k_{\perp} -cutoff is needed. (With the expression in eq. (6) a negative contribution would be obtained for gluons with $k_{\perp} < m_0$.) This generalized measure λ can be used in Monte Carlo simulations of the QCD cascade, where recoils and kinematical constraints are properly taken into account [6, 7]. The recoils are neglected in the strong ordering approximation which led to eqs. (8,9).

We see that for a fixed energy W the perturbative cascade gives a parton state with definite parton momenta, and thus a definite value of λ . The soft hadronization mechanism then gives a certain hadronic state with a hadron multiplicity n . If the hadronization is described by the Lund string fragmentation model, we then find that the distribution in n depends **only on** λ and not on W [6]. Thus for a high energy event with few gluons and a low energy event with many gluons, but with the same λ , we have the same effective string length and the same hadron multiplicity distribution.

It is then possible to separate the multiplicity fluctuations in two pieces

$$\frac{D^2(n)}{\langle n \rangle^2} \Big|_{\text{fixed } W} = \frac{D^2(\lambda)}{\langle \lambda \rangle^2} \Big|_{\text{fixed } W} + \frac{D^2(n)}{\langle n \rangle^2} \Big|_{\lambda=\langle \lambda \rangle} \quad (11)$$

where the first term on the right hand side depends only on the perturbative cascade and the second term only on the soft hadronization. The results are shown in fig. 5. We note that the cascade contribution to the variance, V_{casc} dominates at high energies while the fragmentation contribution, V_{frag} , is more important at lower energies.

We also note that the total variance is essentially proportional to $\langle n \rangle^2$, although this is not the case for the cascade or the fragmentation contribution separately. Thus the full distribution satisfies approximate KNO-scaling.

For the momentum distribution of the hadrons it turns out that it is possible to generalize the hyperbolae in the $q\bar{q}$ - and $q\bar{q}g$ -cases (figs. 4a,b) and define a timelike curve in energy-momentum space [7]. This curve (which we call the x-curve) follows the (colour ordered) parton momenta in such a way that the corners are smoothed out with a resolution power given by a parameter m_0 (see fig. 4c). The length of the x-curve is given by λ and we find that if we just cut it into equal pieces, then we obtain an average momentum distribution of the hadrons. The soft hadronization just adds limited fluctuations around this average.

These features give a quantitative meaning to the notion of local parton-hadron duality (LPHD) [8]. This is illustrated in fig. 6, which shows the distribution in rapidity and transverse momentum at a large energy. We note that if the cutoff is locally invariant, e.g. as a cutoff in dipole mass rather than parton mass, then λ is proportional to the number of gluons and thus $n_{\text{hadrons}} \propto n_{\text{gluons}}$. The x-curve can also be constructed from experimental calorimeter data, as a direct check on the perturbative QCD shower.

2. Fractal Structures and Intermittency in the Perturbative Phase [9]

A. The x-curve has a fractal structure

The x-curve is "longer" if it is studied with a higher resolution. We divide the curve in pieces with a certain invariant length corresponding to a given resolution. If the length of the curve is determined by the number of pieces times the invariant length of each piece, then the total length will decrease with increasing resolution. This is therefore not a suitable way to measure the length of the more twisted curve. Instead we use as definition of the length of a piece with invariant length \hat{s} , the length of a hyperbola passing through the endpoints as shown in fig. 7. This length is given by $\ln(\hat{s}/m_0^2)$ (if \hat{s} is not too small). Thus we define the length S obtained with the resolution given by \hat{s} in the following way

$$S \sim (\text{no of pieces}) \cdot \ln(\hat{s}/m_0^2) \quad (12)$$

Within the analytic approximation discussed above it is possible to calculate S for a given energy s and resolution \hat{s} . The result can be expressed in terms of generalized Bessel functions. For asymptotic energies ($s \gg \hat{s} \gg m_0^2$) we obtain the result

$$S \sim (\ln s)^{1/4} \exp(2\sqrt{\alpha_0 \ln s}) (\ln \hat{s})^{3/4} \exp(-2\sqrt{\alpha_0 \ln \hat{s}}) \quad (13)$$

Thus we see that the fractal dimension D is given by the following expression

$$D = 1 - \frac{d(\ln S)}{d(\ln \hat{s})} \sim 1 + \sqrt{\frac{\alpha_0}{\ln \hat{s}}} = 1 + \sqrt{\frac{3\alpha_s(\hat{s})}{2\pi}} \quad (14)$$

In the square root we recognize the anomalous dimension of QCD. Thus the x-curve gives a geometrical interpretation of this anomalous dimension.

It is possible to calculate $S(s, \hat{s})$ also with the Monte Carlo simulation program, which takes recoils and kinematical constraints better into account. The result is shown in fig. 8 together with the analytic solution given in terms of Bessel functions. The curves are qualitatively similar, although they are quantitatively different. We note in particular that the derivative of $\ln S$ with respect to $\ln \hat{s}$ is decreasing with

increasing \hat{s} , which reflects the running coupling constant in the expression for the dimension in eq. (14). Thus the fractal dimension is also varying and approaching one for very coarse resolutions.

B. Distributions in y and or φ

A lot of interest has recently focused on the notion of intermittency. It was suggested by Białas and Peschanski [10] to study the factorial moments of multiplicity distributions in a rapidity range δy .

$$F_j = \langle n(n-1)\cdots(n-j+1) \rangle / \langle n \rangle^j \quad (15)$$

They suggested that if F_j increases with decreasing δy it is a signal of an intermittent behaviour. For a Poissonic distribution F_j would be independent of δy . In many experiments $\ln F_j$ are seen to rise linearly with $\ln(1/\delta y)$ down to $\delta y \sim 0.1$ and then level off [11].

There are standard methods developed to analyze fractal structures [12]. Let e.g. the total investigated region in y and φ be divided in intervals (in y or φ) or squares (for the 2-dimensional distribution in y and φ) with lengths or sides δ . If the distribution has the scaling property

$$\sum_i n_i^q \sim \delta^\tau \quad (16)$$

where the sum goes over all intervals or squares, then this is interpreted in terms of a dimension D_q given by

$$D_q = \frac{\tau}{q-1} \quad (17)$$

For $q = 0$ the dimension D_0 equals the Hausdorff dimension. (The use of these multifractal dimensions to analyze multiplicity distributions was suggested independently (as far as I know) in Lund, Vienna and Oregon [13].)

If we use normal moments as in eq. (16), or scaled normal moments

$$C_q \sim \frac{\langle n^q \rangle}{\langle n \rangle^q} \quad (18)$$

rather than the factorial moments in eq. (15), then it is possible to study also noninteger variables, e.g. the piece of the x-curve which has its tangent within an interval in y and/or φ .

As an example fig. 9 shows moments obtained for the x-curve when binned in y -intervals, using the ARIADNE MC for e^+e^- -annihilation at 200 GeV. The corresponding dimensions D_q are shown in fig. 10 together with corresponding results obtained from a binning in φ and from a twodimensional distribution in y and φ . We note from the figure the surprising result that the dimensions are **essentially the same in all three cases**. The reason for this is not understood. Could it be an effect of a stringlike behaviour, such that the projection of the x-curve on the $y - \varphi$ plane has a fractal dimension along the curve and dimension 0 perpendicular to it?

C. Hadron distributions

Let us assume that there are events of different types such that each type corresponds to a fixed average multiplicity $\bar{n} = \rho \delta y$ in one bin and that for this type of events there is a Poisson distribution around this average. If the different types correspond to a distribution $f(\bar{n})$ then the normal multiplicity moments blow up for small δy while the factorial moments F_q are given by

$$F_q \sim \int \bar{n}^q f(\bar{n}) d\bar{n} \quad (19)$$

Thus if the underlying dynamics determines $f(\bar{n})$, then one should look at the factorial moments, as was suggested by Białas and Peschanski [10].

This can be compared to the situation described above where the perturbative QCD cascade gives a partonic state corresponding to a certain x-curve, and the soft hadronization process gives a number of hadrons fluctuating around an average determined by the parton state. However, in string fragmentation the fluctuations are smaller than in a Poisson distribution, the variance V is approximately equal to $\frac{2}{3}V_{\text{Poisson}}$. Furthermore, the production of particles in neighbouring bins are correlated.

In fig. 11 is shown both normal moments and factorial moments for the hadron distribution, compared with the moments from the x-curve. We see that indeed the

normal moments shoot up above the x-curve for small δy but that they nevertheless are closer to the x-curve than the factorial moments, which are much further below. It is at present not quite clear if this also implies that the normal moments are more related to the underlying dynamics of perturbative QCD, or if one could find some other quantity which interpolates between the normal and factorial moments, and which would be even better.

3. Intermittent Effects in Soft Hadronization [14]

I will here not discuss the question whether the rising factorial moments are indications for a basic intermittent structure. In many experiments on e^+e^- -annihilation [15, 16] and other reactions [11] $\ln F_q$ rises with $\ln(1/\delta y)$ with a steeper slope than Monte Carlo calculations based on Lund string fragmentation [17] or the Webber cluster model [18]. Thus one may wonder if these models are basically wrong.

These models are tuned to fit other variables, and are not retuned to reproduce the intermittency slopes. We have found that in the Lund model a large part of the effect is due to directly produced pions which are neighbours in rank (i.e. pions which are not decay products of ρ 's, ω 's and other resonances). This implies that the result is very sensitive to the vector to pseudoscalar ratio. The default value in the MC is $P/(V + P) = 0.5$, and we note that e.g. the probability to have three directly produced pions in a row is proportional to $(P/(V + P))^3$. We also note that the vector meson production measured by the NA22 collaboration [19] is smaller than the corresponding MC results.

This observation also implies that the result is very sensitive to the fragmentation p_\perp for direct pions, i.e. the p_\perp (with respect to the string direction) given to the pions in the rest frame of the string. In string fragmentation the particles are ordered in rapidity. Thus if p_\perp is smaller the particles are not only closer in p_\perp but also closer in p_L .

The production of $q\bar{q}$ pairs in the string can be described as a tunnelling process [20]. Classically the quark and the antiquark are produced at a certain distance $2\mu_\perp/\kappa$, and then pulled apart by the string force. Here μ_\perp is the transverse mass of the quark (and antiquark) and $\kappa \sim 0.2 \text{ GeV}^2$ is the string tension. Quantum mechanically the quark wavefunction has a tail out in the classically forbidden region, and the production probability is given by the overlap between the quark and the antiquark wavefunctions in this region.

The suppression of the wave functions from the classical boundaries to the overlap

region can be estimated using the WKB method, and gives the following factor for the production probability

$$Prob. \sim \exp\left(-\frac{\pi}{\kappa}\mu_{\perp}^2\right) = \exp\left(-\frac{\pi}{\kappa}\mu^2\right)\exp\left(-\frac{\pi}{\kappa}k_{\perp}^2\right) \quad (20)$$

where k_{\perp} is the transverse momentum of the quark and the antiquark and μ is their mass.

This would be the whole story for quarks pulled off to infinity by the string. In practice the quark must join an antiquark from a neighbouring pair and form a mesonic bound state. For different mesons we obtain from normalization different values for the wavefunction at the classical boundary, and therefore also at the production point in the classically forbidden region. This effect was estimated in ref. [21]. The result was that the probability for a quark to fit into a bound state meson wave function is approximately proportional to $(m_{\perp})^{-1}$ where m_{\perp} is the transverse mass of the meson.

$$Prob. \text{ to fit into mesonic wave function} \sim \frac{1}{m_{\perp}} \quad (21)$$

In ref. [21] this result was used to understand the suppression of vector mesons relative to pseudoscalar mesons. The ratio between ρ and π seems to be of the order 1 : 1 rather than 3 : 1 as obtained from spin counting. For heavier mesons, as e.g. D and D^* , the mass difference is not so large and we therefore do not expect such a suppression, in good agreement with data.

In the MC program $q\bar{q}$ pairs are produced with a common Gaussian k_{\perp} distribution, as obtained from eq. (20). For most mesons the k_{\perp} -dependence in eq. (21) is also very small compared to this Gaussian distribution. For pions, which have a very small mass, this is however not the case, and we thus expect that the directly produced pions have smaller transverse momenta than other mesons. Because most pions are the decay products of ρ 's, ω 's and other resonances, this effect is not noticeable in most observables, the intermittency being one exception.

We note that we get one factor $(m_{\perp})^{-1}$ in eq. (21) from each quark or antiquark. Thus we also have correlations between neighbouring hadrons. A $q\bar{q}$ pair with small k_{\perp} has an increased probability to go into two neighbouring pions. The direct pions thus have a tendency to come in bunches, which increases the intermittency further.

We do not yet have a Monte Carlo program which takes this effect properly into account. However, in fig. 12 we show results where we have assumed that the direct pions are produced with $p_{\perp} = 0$ with respect to the string and that the vector mesons are suppressed so that $V/(V + P) = 0.3$. This is of course an exaggeration, but it can teach us the order of magnitude of the effect.

We note, however, that the TASSO data shown in fig. 12 are not corrected. When the MC generated events are processed through the detector simulation, the result is increased [15]. Thus the full difference between the old MC results and the data is not dynamical. We also note that the MC does not include the Bose-Einstein effect. This effect must increase the slopes of the factorial moments.¹ It can not be the dominant effect, however, because it would give a larger signal for same sign particles than for all charged particles, in contradiction with the data [15, 22]. Direct charged pions which are neighbours in rank must have opposite charges. Thus the effect discussed above is largest for particles of opposite charges.

We conclude that with about equal contributions from detector acceptance, Bose-Einstein interference and the effect from directly produced pions discussed here, it is likely that we can satisfactorily describe the difference between the MC simulations and the data in fig. 12.

Although not noticeable in most other variables, the effect discussed here should be observable also in the K/π ratio at high p_{\perp} in hadronic collisions. The ABCDHW collaboration at ISR [23] has observed a higher K^+/π^+ ratio than what is obtained in the MC calculations. Due to the trigger bias effect this ratio is most sensitive to the jet fragmentation for large values of z and thus to the directly produced pions and kaons. As the experiment is measuring at an angle $\theta \sim 50^\circ$ a smaller p_{\perp} with respect to the jet direction will result in a smaller p_{\perp} also with respect to the beam direction, and therefore to an increased K/π ratio. As a smaller p_{\perp} in the Lund model implies also a smaller p_L , we see that the K/π ratio will be enhanced also at $\theta \sim 90^\circ$ although to a somewhat lesser degree.

We are presently working on a modification of the Monte Carlo program in order to fully check that it is possible to simultaneously reproduce the previously well reproduced observables, the intermittency, the vector meson production and the K/π ratio at large p_{\perp} .

We finally note that the effects discussed here should be noticeable not only in e^+e^- .

¹A MC version in which identical pairs are pulled together to reproduce the Bose-Einstein correlation is produced by T. Sjöstrand. This MC indeed gives an increased intermittency effect [24].

annihilation, but also in DIS and hadronic collisions if the particles also here are produced from a stringlike colour field

4. Conclusions and Comments

Fractals and intermittency are new tools to study multiparticle dynamics. QCD is a nonlinear theory, and we therefore expect fractal structures. QCD is also not scaling, the coupling constant α_s is running, and thus we should expect the fractal dimensions to vary with energy and resolution. To understand these properties, it is very essential to have both a Monte Carlo simulation program and approximation methods suitable for analytic analyses.

A. For the **hard perturbative phase** of QCD we have found the following properties.

- The so-called **x-curve** is defined on a parton state and gives the average momentum distribution of the final hadrons. It is a **fractal curve**, embedded in fourdimensional energy-momentum space. If suitably defined the length increases with the resolution according to a dimension $D = 1 + \sqrt{\frac{3\alpha_s}{2\pi}}$. In the square root we recognize the anomalous dimension of QCD, and thus the x-curve provides a geometrical interpretation of this anomalous dimension. We also note that the dimension varies with the resolution in accordance with the running coupling constant α_s .

- For the **distributions in y and φ** we note that it is possible to study moments, not only for multiplicity but also for continuous variables like e.g. the piece of the x-curve with tangent within a certain angular region. We then note that the corresponding multifractal dimensions D_q are the same whether we bin in y or in φ or do a twodimensional analysis in y and φ . The reason for this feature is not clear; could it be an effect of a stringlike behaviour?

- For the **hadronic multiplicity** we note that the normal moments, as expected, go above the moments of the continuous x-curve for small δy , but that they nevertheless are closer to the x-curve results than the factorial moments, which are much further below. Does this mean that the normal multiplicity moments also are closer to the dynamical structure of QCD, as the x-curve is defined directly from the parton state?

B. For the **soft hadronization phase** we have observed that in the Lund string fragmentation model the intermittency signal is most sensitive to directly produced pions which are neighbours in rank. From the $q\bar{q}$ tunnelling mechanism we expect that direct pions have smaller p_{\perp} than other hadrons. This effect is neglected in the

MC. It is unessential in most observables but noticeable in the intermittency signal and in the K/π ratio at high p_{\perp} in hadron collisions. We expect that this effect together with Bose-Einstein interference can account for the discrepancy between data and MC results for the intermittency signal.

C. Hopes for the future

The x-curve is a fractal curve embedded in fourdimensional space, with a fractal dimension $D = 1 + \sqrt{\frac{3\alpha_s}{2\pi}}$, which is larger than 1. The distribution in y or φ correspond to multifractal dimensions D_q , which are smaller than 1 (for $q > 0$). What is the relation between these dimensions? I would like to see analytic results for D_q in QCD (not only MC results or toy models) in order to understand the dynamical structure.

For the soft phase we would like to have the description in terms of probabilities replaced by a quantum mechanical description in terms of amplitudes. In this process we may hope that an understanding of the intermittency signal can be helpful as it seems to be related to quantum mechanical effects like Bose-Einstein interference, the tunnelling of $q\bar{q}$ -pairs or perhaps quantum optics.

References

- [1] G. Gustafson, *Phys. Lett.* **B175** (1986) 453
G. Gustafson, U. Pettersson, *Nucl. Phys.* **B306** (1988) 746
- [2] B. Andersson, P. Dahlqvist, G. Gustafson, *Phys. Lett.* **B214** (1988) 604
- [3] Ya.I. Azimov, Yu.L. Dokshitzer, V.A. Khoze, S.I. Troyan, Coherence effects in QCD jets, Leningrad preprint 1051 (1985); *Phys. Lett.* **B165** (1985) 147
- [4] L. Lönnblad, U. Pettersson, ARIADNE 2 - A Monte Carlo for QCD Cascades in the Colour Dipole Formulation - an update, Lund preprint LU TP 88-15
- [5] A.H. Mueller, *Nucl. Phys.* **B213** (1983) 85, **B228** (1983) 351
A. Bassetto, M. Ciafaloni, G. Marchesini, *Phys. Rep.* **100** (1983) 201
- [6] B. Andersson, P. Dahlqvist, G. Gustafson, *Z. Physik* **C44** (1989) 455
- [7] B. Andersson, P. Dahlqvist, G. Gustafson, *Z. Physik* **C44** (1989) 461
- [8] Ya.I. Azimov, Yu.L. Dokshitzer, V.A. Khoze, S.I. Troyan, *Z. Physik* **C27** (1985) 65

L. van Hove, A. Giovannini, CERN preprint TH 4885/87
M. Garretto, A. Giovannini, T. Sjöstrand, L. van Hove, CERN preprint TH 5252/88

- [9] G. Gustafson, A. Nilsson, in preparation
- [10] A. Bialas, R. Peschanski, *Nucl. Phys.* **B273** (1986) 703, **B308** (1988) 857
- [11] For a review, see e.g. W. Kittel, R. Peschanski, *Proceedings of the 1989 EPS Conference*, Madrid, 1989. (Saclay preprint SPhT/89-143)
- [12] See e.g. T. Halsey et al., *Phys. Rev.* **A33** (1986) 1141
- [13] P. Dahlqvist, G. Gustafson, B. Andersson, *Nucl. Phys.* **B328** (1989) 76, Proc. of XXIV Rencontre de Moriond, March 1989,
P. Lipa, B. Buschbeck, *Phys. Lett.* **B223** (1989) 465, Proc. of XXIV Rencontre de Moriond, March 1989
R.C. Hwa, Univ. of Oregon preprint OITS407 (March 1989)
- [14] G. Gustafson, C. Sjögren, in preparation
- [15] W. Braunschweig et al. (TASSO), *Phys. Lett.* **B231** (1989) 548
- [16] B. Buschbeck, P. Lipa, R. Peschanski (HRS data), *Phys. Lett.* **B215** (1988) 788
K. Sugano (HRS), talk presented at this conference
- [17] B. Andersson, G. Gustafson, G. Ingelman, T. Sjöstrand, *Phys. Rep.* **97** (1983) 31
T. Sjöstrand, *Computer Phys. Comm* **39** (1986) 347
T. Sjöstrand, M. Bengtsson, *Computer Phys. Comm* **43** (1987) 367
- [18] B.R. Webber, *Nucl. Phys.* **B238** (1984) 492
G. Marchesini, B.R. Webber, *Nucl. Phys.* **B238**(1984) 1
- [19] NA22 Collaboration, to be published in *Z. Physik C*
- [20] B. Andersson, G. Gustafson, T. Sjöstrand, *Z. für Physik C6* (1980) 235
- [21] B. Andersson, G. Gustafson, Lund preprint LU TP 82-5
- [22] I.V. Ajinenko et al. (NA22), contrib. to the EPS conference, Madrid 1989
- [23] A. Breakstone et al., *Phys. Lett.* **B135** (1984) 510
- [24] W. Kittel, this conference

Perturbative phase

Soft phase

clusters or string

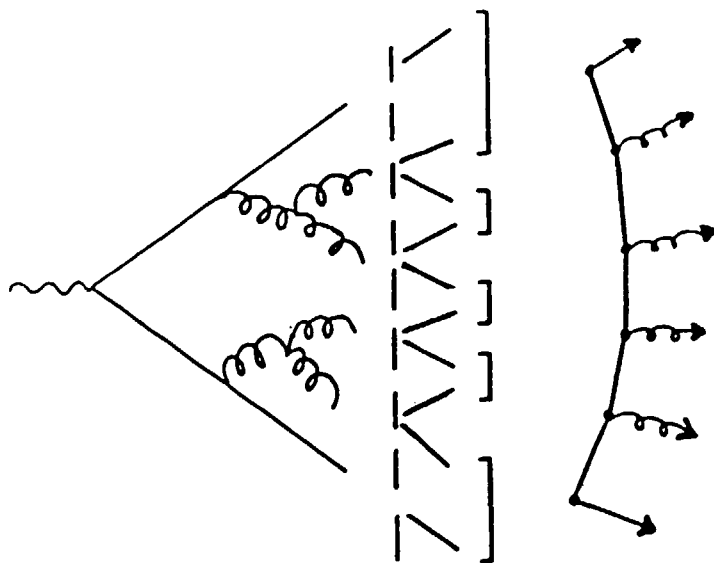


Fig. 1. The e^+e^- -annihilation process is divided in a short-time, perturbative and a long-time soft phase. The latter can be described either by a string or by cluster formation.

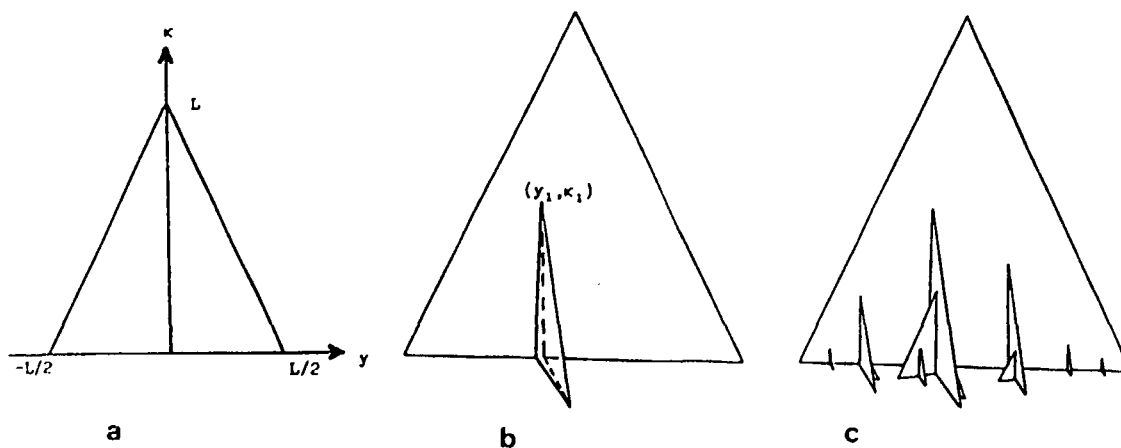


Fig. 2a. The phase space available for a gluon emitted by a high energy $q\bar{q}$ system is a triangular region in the $y - \kappa$ plane ($\kappa = \ln k_T^2/\Lambda^2$).

Fig. 2b. If one gluon is emitted at (y_1, κ_1) the phase space for a second (softer) gluon is represented by the area of this folded surface.

Fig. 2c. Each emitted gluon increases the phase space for the softer gluons. The total gluonic phase space can be described by this multifaceted surface.

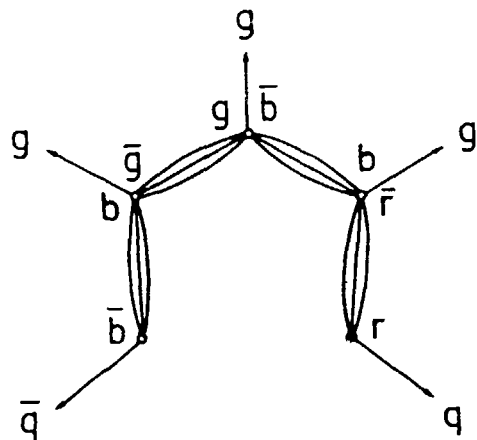


Fig. 3. A system of a quark, an antiquark and n gluons emit further soft gluons like $n + 1$ dipoles. These dipoles connect the gluons in the same way as the string in the string model.

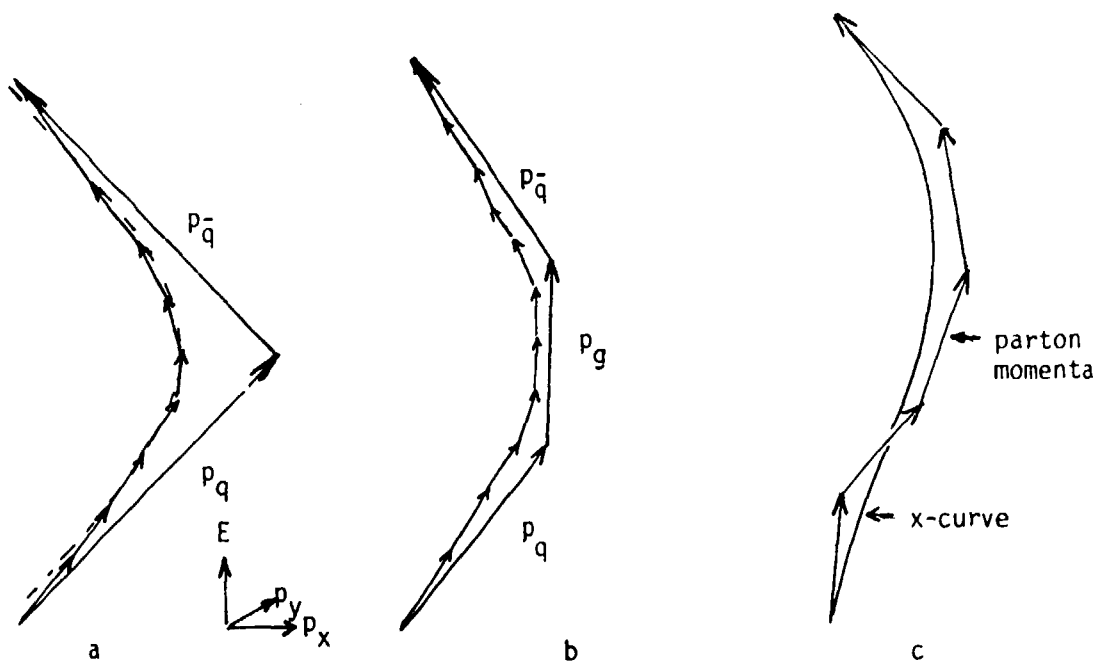


Fig. 4a. In a $q\bar{q}$ system the hadron momenta are distributed around a hyperbola in energy-momentum space.

Fig. 4b. For a $q\bar{q}g$ -system the hadron momenta are distributed around two hyperbolae.

Fig. 4c. For a multigluon state the hadron momenta are distributed around a curve in energy-momentum space (called the x-curve) which smoothly follows the (colourordered) parton momenta.

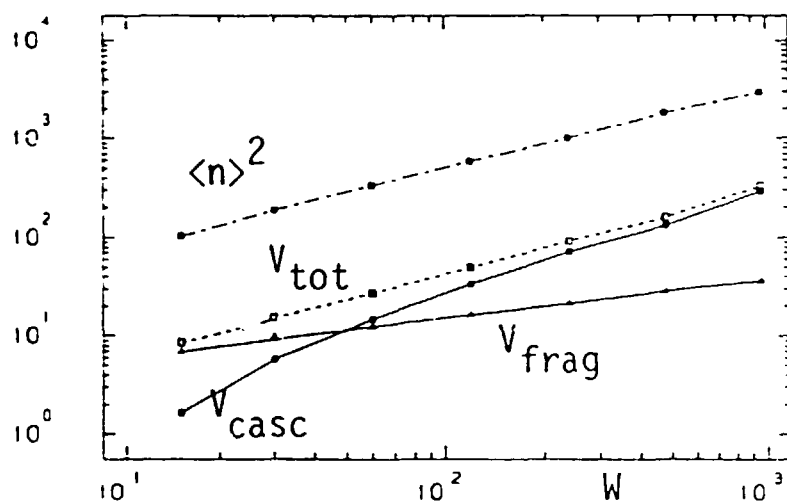


Fig. 5. The variance, V , separated into contributions from the QCD cascade, V_{casc} , and the soft fragmentation, V_{frag} . The dash-dotted curve shows $\langle n \rangle^2$.

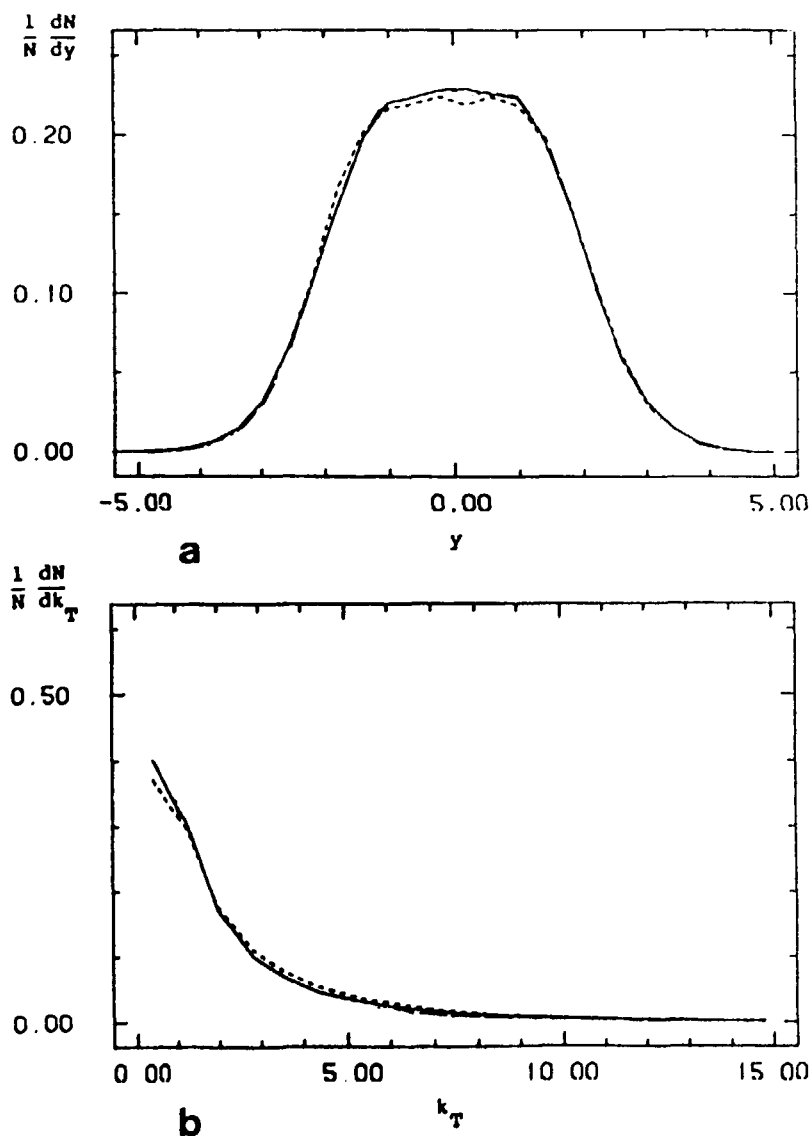


Fig. 6. Distributions in rapidity (a) and p_T (b) for e^+e^- -annihilation events at 200 GeV with sphericity > 0.1 . The dashed curve corresponds to a partitioning of the x-curve and the solid line to standard Lund fragmentation.

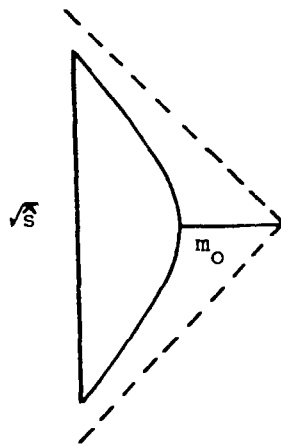


Fig. 7. The "length" of a piece with invariant length \sqrt{s} is defined as the length of a hyperbola passing through the endpoints.

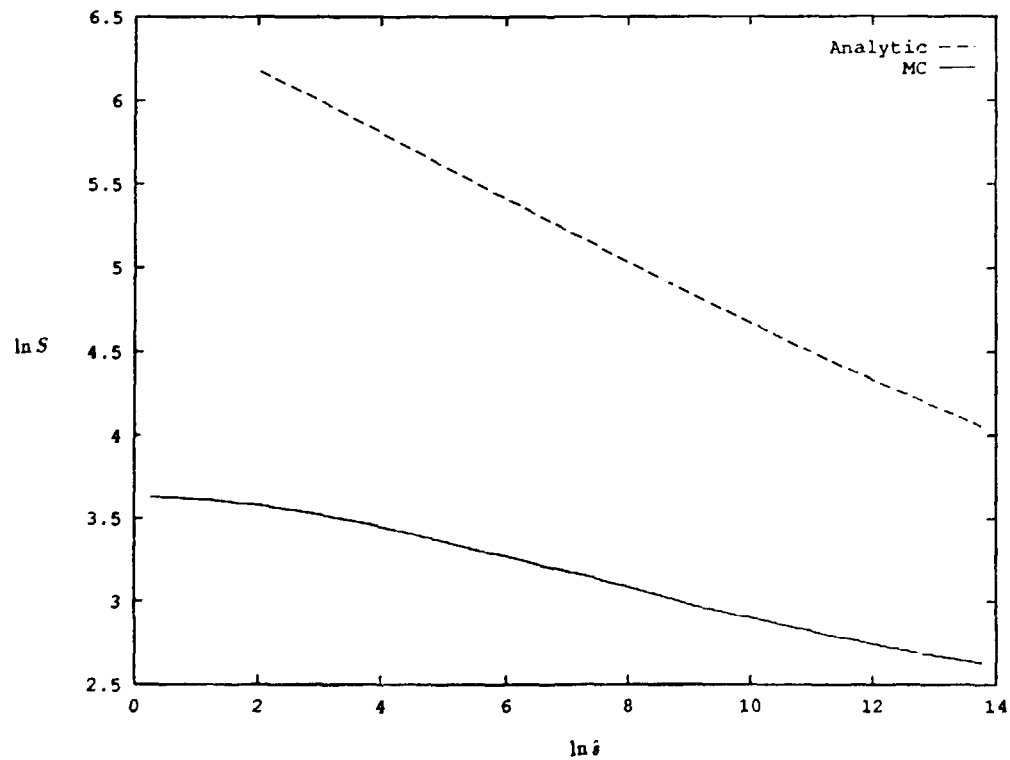


Fig. 8. The length S of the x-curve, as defined in eq. (12), as a function of the resolution δ , in e^+e^- -annihilation at 1000 GeV. The solid line is the analytic approximation and the dashed line shows the MC results.

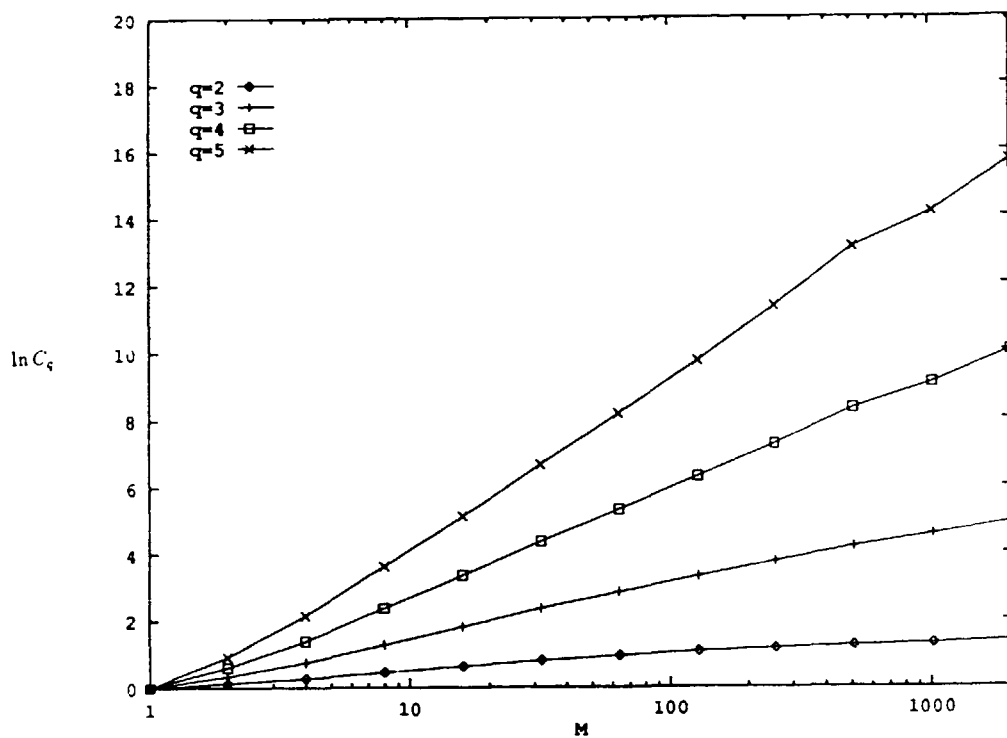


Fig. 9. Normalized moments C_q for the x-curve pieces within varying rapidity regions δy . The energy is 200 GeV and the total y-range studied is $-2 < y < 2$. $M = 4/\delta y$ is the number of bins.

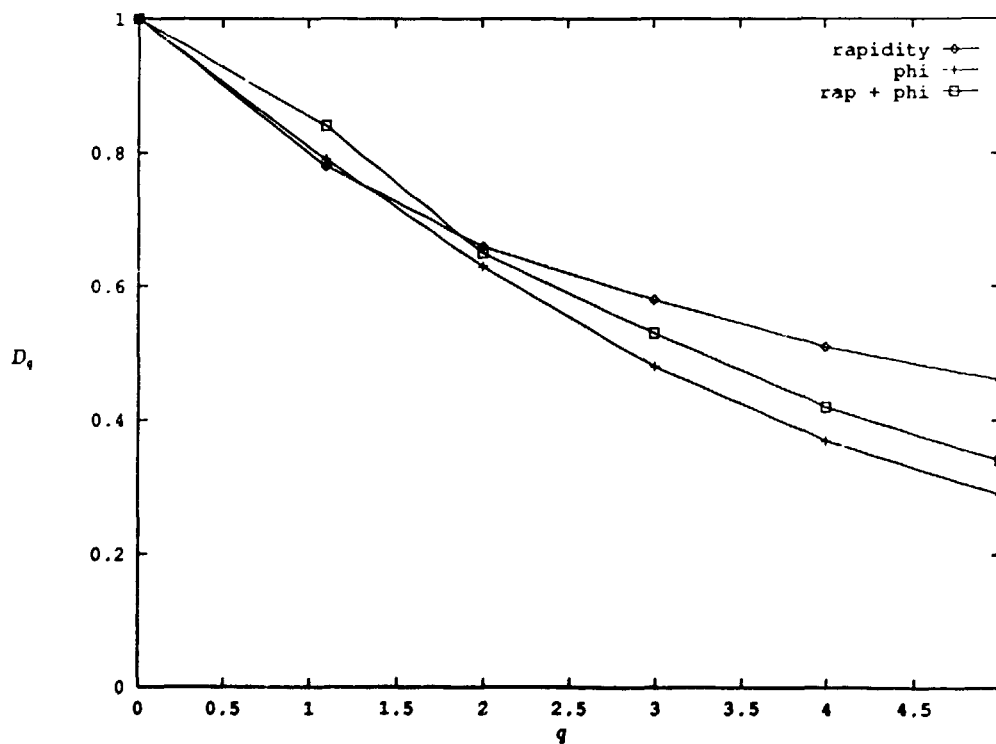


Fig. 10. Multifractal dimensions D_q from moments of the x-curve when binned in y , in φ or simultaneously in y and φ . The energy is 1000 GeV.

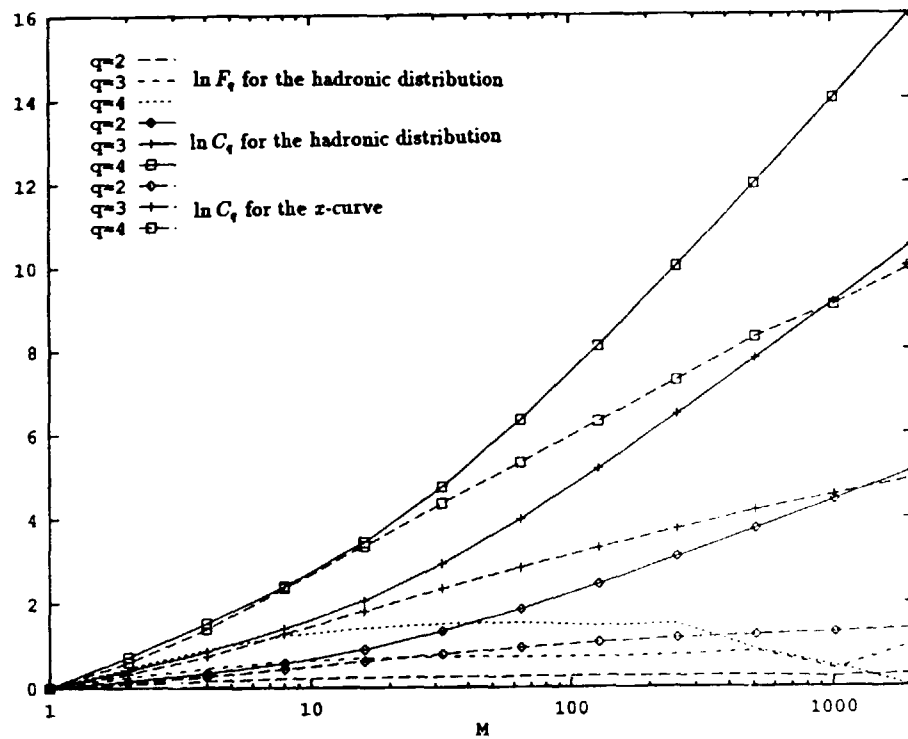


Fig. 11. Normal moments C_q and factorial moments F_q for the hadron distribution, compared with the moments of the x-curve from fig. 9.

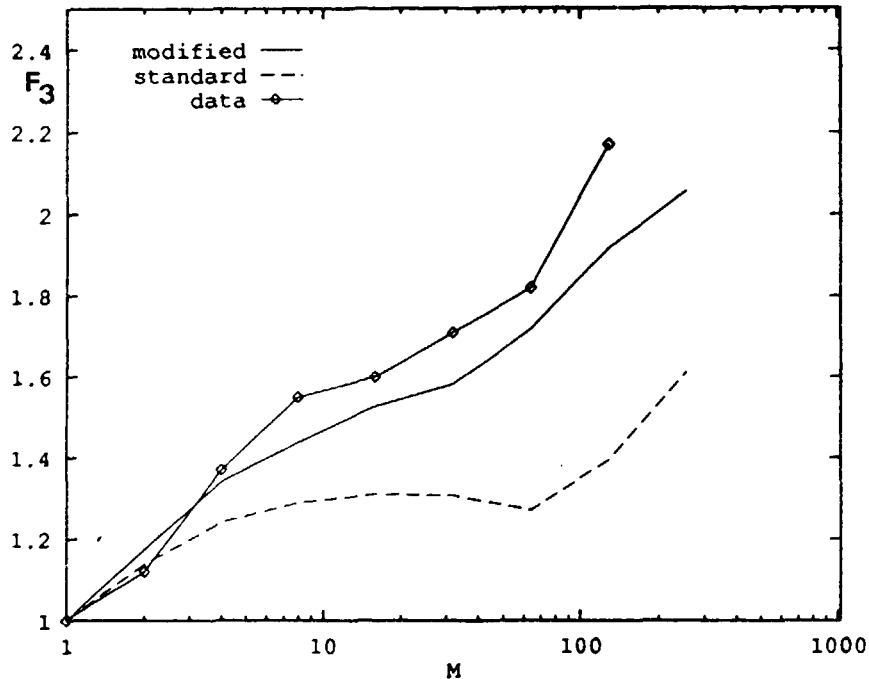
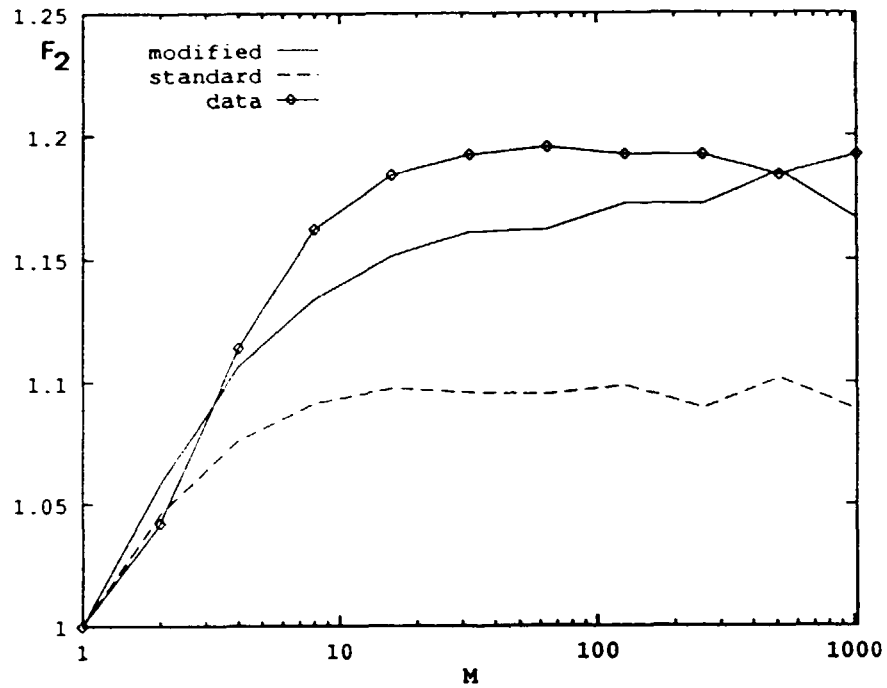


Fig. 12. Normalized factorial moments F_2 and F_3 for e^+e^- -annihilation at 36 GeV. The squares are the uncorrected data from TASSO [15], the dashed lines show results from the ARIADNE MC with default values for the parameters. The solid lines show results where $V/(V + P) = 0.3$ and the directly produced pions have $p_{\perp} = 0$ with respect to the string. (The results would be similar with Sjöstrand's MC version for the QCD cascade [17]. Both Monte Carlos use the same program for the Lund string fragmentation.)